10.3 Background Error Covariance Functions for Radar Wind Analysis

Qin Xu*, National Severe Storms Laboratory, Norman OK
Jiandong Gong, CIMMS, University of Oklahoma, Norman OK

1. Introduction

Modern Doppler radars have the ability to scan large volumes of the atmosphere at high spatial and temporal resolutions, but the wind measurements are limited to the velocity component in the radial direction of the radar beam. When radial-wind measurements are analyzed and interpolated on to a regular grid for numerical applications, there is a question concerning whether radial winds can be treated as scalars as in many existing schemes for Doppler radar radial-wind analyses. This question is addressed in this paper.

2. Error covariance functions

Denote by $\mathbf{v} = (u, v)$ the error field of background wind and assume that $\mathbf{v}$ is an unbiased Guassian random vector field in the horizontal. The radial component of $\mathbf{v}$ at point $\mathbf{x}_i = (x_i, y_i)$ viewed from the radar (located at the origin) can be expressed by

$$v_{ri} = u_i\cos\beta_i + v_i\sin\beta_i. \quad (1)$$

Using (1) and (5.2.18) of Daley (1991), one can derive the covariance function of v_r, that is,

$$\begin{aligned} &C_{vr}(\mathbf{x}_1, \mathbf{x}_2) = \langle v_{r1}v_{r2}\rangle \\ &= \langle(u_1\cos\beta_1 + v_1\sin\beta_1)(u_2\cos\beta_2 + v_2\sin\beta_2)\rangle \\ &= 0.5[C_{ll}(r) + C_{tt}(r)]\cos(\beta_1 - \beta_2) \\ &\quad + 0.5[C_{ll}(r) - C_{tt}(r)]\cos(\beta_1 + \beta_2 - 2\alpha), \end{aligned} \quad (2)$$

where $\langle(\bullet)\rangle$ denotes the mean of $(\bullet)$, $C_{ll}(r) = \langle l_1 l_2\rangle$, $C_{tt}(r) = \langle t_1 t_2\rangle$, $r = |\mathbf{x}_1 - \mathbf{x}_2|$, $(l_i, t_i)^T = \boldsymbol{R}\mathbf{v}_i$ $(i = 1, 2)$, $\boldsymbol{R} = \boldsymbol{R}(\alpha)$ is the rotational matrix that rotates the x-axis to the l-direction (from $\mathbf{x}_1$ to $\mathbf{x}_2$), α is the angle of the rotation, β_1 and β_2 are the direction angles of $\mathbf{x}_1$ and $\mathbf{x}_2$, respectively (positive for counterclockwise, see Fig. 1).

The covariance functions estimated for 850 mb in Fig. 1 of Xu and Wei (2001) can be approximated by

$$\begin{aligned} &C_{ll}(r) + C_{tt}(r) = 2\sigma^2\exp[-r^2/(2L^2)], \\ &C_{ll}(r) - C_{tt}(r) = (\sigma_r^2 - \sigma_d^2)r^2L^{-2}\exp[-r^2/(2L^2)], \end{aligned} \quad (3)$$

where $2\sigma^2 = \sigma_r^2 + \sigma_d^2$ is the variance of $\mathbf{v}$ with σ_r^2 for the rotational part and σ_d^2 for the divergent part, and L is the decorrelation length scale. In this paper, L is downscaled to 12 km.

* *Corresponding author address:* Qin Xu, NSSL/NOAA, 1313 Halley Circle, Norman, OK 73069; e-mail: Qin.Xu@nssl.noaa.gov.

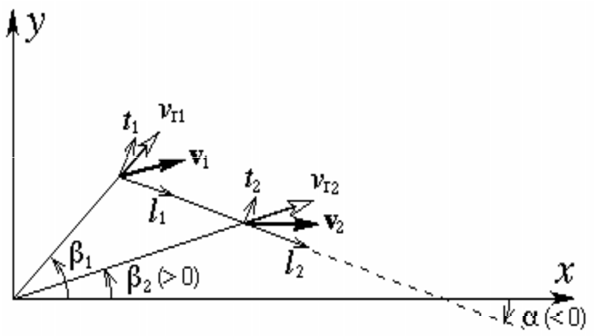

Fig. 1. Velocity vectors (bold arrows $\mathbf{v}_1$ and $\mathbf{v}_2$), their radial components (hollow arrows v_{r1} and v_{r2}), l-components (thin arrows l_1 and l_2), and t-components (thin arrows t_1 and t_2).

3. Analysis of a single observation

When the statistic interpolation is applied to a single radial-wind observation at point $\mathbf{x}_1$, the observation space becomes one-dimensional and the increment field produced by a single observation has the same structure as the correlation function defined by $C_{vr}(\mathbf{x}_1, \mathbf{x})/\sigma^2$. An example is shown in Fig. 2.

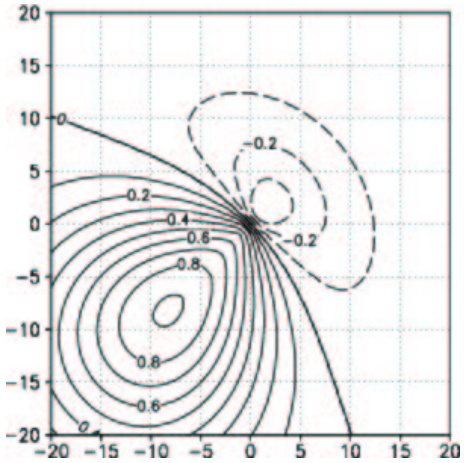

Fig. 2. Correlation function $C_{vr}(\mathbf{x}_1, \mathbf{x})/\sigma^2$ for $\mathbf{x}_1 = (x_1, y_1) = (-6, -6)$ km, $L = 12$ km and $\sigma_r^2/\sigma_d^2 = 1.5$.

Note that $\beta - \beta_1$ is the angle of vector $\mathbf{x}$ with respect to vector $\mathbf{x}_1$ and $\alpha - \beta_1$ is the angle of vector $\mathbf{x} - \mathbf{x}_1$ with respect to vector $\mathbf{x}_1$ (see Fig. 1 but with $\mathbf{x}_2$ viewed as $\mathbf{x}$). This implies that $\cos(\beta_1 - \beta_2)$ and $\cos(\beta_1 + \beta_2 - 2\alpha)$ in (2) are invariant for a mirror reflection of $\mathbf{x}$ with respect to vector $\mathbf{x}_1$ (along the diagonal line of y = x), and so does the correlation function in Fig. 2.

As shown in Fig. 2, $C_{vr}(\mathbf{x}_1, \mathbf{x})$ is positive and approaches to unity as $r = |\mathbf{x} - \mathbf{x}_1|$, but it becomes negative as $\mathbf{x}$ moves to the northeast of the radar across the zero contour. This change of sign is consistent with the continuity of the vector wind field inferred from a single (positive) observation at $\mathbf{x}_1$ (where the observed radial wind is southwestward away from the radar).

6. Numerical Experiments

The true wind field is assume to be uniform with U = 1 m s^{-1} and V = 1 m s^{-1}. The true radial wind is given by $U\cos\beta + V\sin\beta$ (Fig. 3). The observed radial winds are given on a polar grid centered at the radar with resolutions of 1 km in the radial direction and 1 degree in the azimuthal direction, but cover only the left half of the domain outside the 10 km range of the radar (shown by the shaded area in Fig. 3). The observation error is measured by σ_{ob} = 1 m s^{-1}. The background field is assumed to be zero but the background error is nonzero with σ = 10 m s^{-1}.

The analysis (statistic interpolation) with the correlation function in (2)-(3) is plotted in Fig. 4. As shown, the analysis is very close to the true radial-wind field within the data dense area in the left-half domain, except for the southwest corner area where the radial wind is underestimated due to the lack of observations outside of the domain. The true radial-wind field is symmetric with respect to the radar (Fig. 3). This symmetry is well captured by the analyzed field in the vicinity of the radar within the range of the decorrelation length scale (12 km) including the data void area in the right-half domain.

Figure 5 is the analysis performed by using the same method as in Fig. 4 but with the following isotropic correlation (obtained by treating radial winds as scalars):

$$C_{vr}(\mathbf{x}_1, \mathbf{x})/\sigma^2 = \exp[-r^2/(2L^2)]. \qquad (4)$$

The analysis obtained with (4) is quite different from the true radial-wind field especially in the vicinity of the radar. Numerical experiments are also performed with real Doppler data and the results will be presented at the conference.

Acknowledgments: The research work was supported by FAA contract IA# DTFA03-01-X-9007 to NSSL, and by ONR Grants N000140210452 and N000140210453 to the University of Oklahoma.

REFERENCES

Daley, R., 1991: *Atmospheric Data Analysis*. Cambridge University Press, 457 pp.

Xu, Q., and L. Wei, 2001: Estimation of three-dimensional error covariances. Part II: Analysis of wind innovation vectors. *Mon. Wea. Rev.*, **129**, 2939-2954.

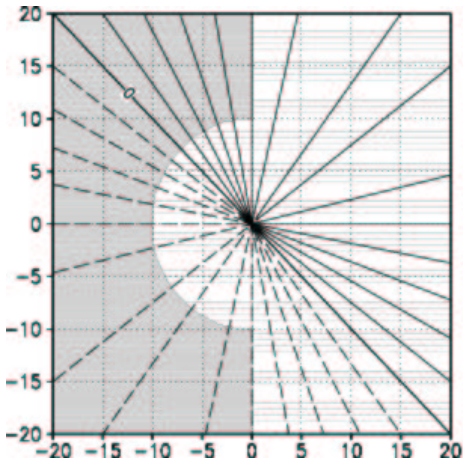

Fig. 3. Idealized true radial wind field: $U\cos\beta + V\sin\beta$.

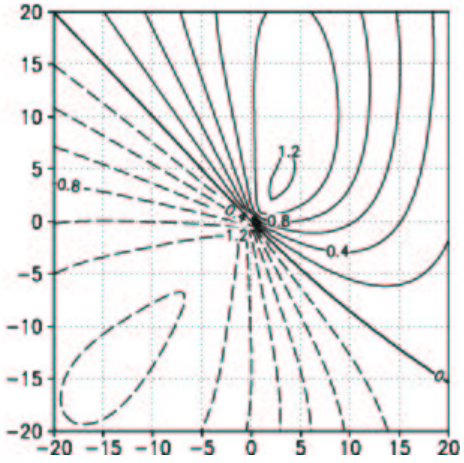

Fig. 4. Analyzed radial wind field using (2)-(3) with L = 12 km and σ_r^2/σ_d^2 = 1.5.

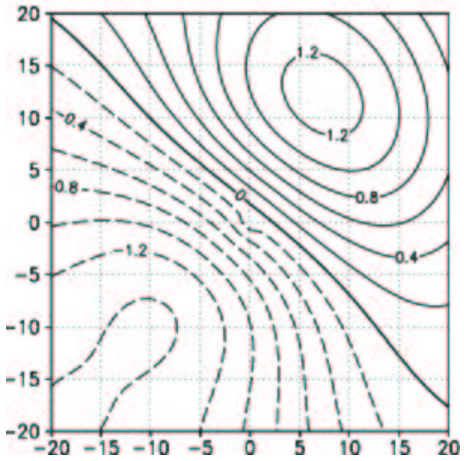

Fig. 5. As in Fig. 4 but using (4) with L = 12 km.